A Multiport Bidirectional LLC Resonant Converter for Grid-Tied Photovoltaic-Battery Hybrid System

Garry Jean-Pierre[1], Ahmad El Shafei[1], Necmi Altin[1,2], and Adel Nasiri[1]

[1]Center for Sustainable Electrical Energy Systems, University of Wisconsin Milwaukee, Milwaukee, USA
[2] Department of Electrical & Electronics Engineering, Faculty of Technology, Gazi University, Ankara, Turkey
jeanpie4@uwm.edu; aie@uwm.edu; naltin@gazi.edu.tr; nasiri@uwm.edu

Received: 10.04.2020 Accepted:22.06.2020

Abstract- Distributed power generation plants with combined photovoltaic (PV) systems and integrated energy storage for grid-connected applications have seen an increase in research interest in recent years. However, the combination of multiple energy sources requires numerous DC-DC converters and thus becomes more complex. To address this issue, a multiport bidirectional DC-DC LLC resonant converter for grid connected applications is presented in this research. In order to minimize the control complexity of the proposed system, a zone based controller approach with an integrated modified maximum power point tracking (MMPPT) method, which is based on the incremental conductance method, is also developed. This proposed controller is able to regulate the converter voltage and power flow while either delivering or taking power from the utility grid. The converter presented in this study contains a bidirectional buck-boost converter and an LLC resonant converter in addition to a voltage source grid-tied inverter. These all interface with the PV, the battery and the utility. Extensive simulation analyses through MATLAB/Simulink have proved the operations of the proposed topology.

Keywords: Multiport converter, PV-battery hybrid system, Bidirectional LLC resonant converter, MPPT.

1. Introduction

Power electronic converters and control methodologies have seen tremendous growth in power distribution systems in order to achieve sustainable transmission networks. Therefore, some key design elements have arisen, such as compactness, high power capability and higher efficiency. Managing multiple energy sources, such as wind, PV, battery and fuel cell, through a single power electronic converter becomes the new research and industry applications trend. Numerous converter topologies have been presented in the literature and they can be classified into two main categories: unidirectional and bidirectional converters. The unidirectional converter has been extensively studied. Despite presenting many good features, in the standalone applications it is not well suited for achieving compactness, especially when isolation is a part of the system requirements. Utilizing the unidirectional converter in highly integrated energy sources may increase the number of converters, leading to an increase in size and cost of the system. Additionally, control for power sharing between the converters can be complex and introduce instability into the system, potentially decreasing the efficiency [1]. Therefore, bidirectional converters are a more suitable configuration for multi-energy integration systems. This type of configuration is mainly found in battery storage, uninterruptible power supplies (UPS), motor drives and vehicle to grid (V2G) applications. They also function well in high frequency operations with the use of a high frequency solid state transformer. While this configuration presents many advantages, such as high voltage connection, power density and efficiency [2], [3], further improvements and modifications have been done to increase the number of connected devices through a single converter. This has led to the rise of multiport converter topologies. A half-bridge three-port converter was presented in [4] for connecting renewable energy sources (RES), a battery storage unit and loads. The power flow among the ports of this converter was presented to support the study. To achieve soft-switching, operate at steady state and manage power flow, a three-port DC-DC bidirectional converter with zero voltage switching was studied in [5]. In [6], another three-port configuration was examined for the integration of fuel cell and battery storage systems. Despite the advantages presented by these converters, there are some drawbacks. The usage of the three-winding transformer with three separate converters results in an increase in the complexity, the footprint and the cost of the system.

In order to address these drawbacks, researchers have introduced multiport converters which are configured through two winding transformers. In [7], a new multiport isolated bidirectional DC-DC converter was introduced for hybrid battery storage and super-capacitor system applications. In [8], an altered design of the isolated half-bridge converter structure was presented for interfacing the utility grid, the battery storage and the load port. The three modes of operation were analyzed in order to establish the control parameters for the converter. Another modified representation of the half-bridge converter was introduced in [9] to interface two different sources, a bidirectional battery storage and the isolated output port. The full-bridge converter was then altered

in [10] in order to obtain a three port converter. In that study the derivation methodology and the configuration of the proposed converter were presented.

Increased demand for higher efficiency, power density and frequency operation in more sustainable energy source applications has driven researchers to look for an alternate power converter design to meet these challenges, while keeping the loss at a minimum. Apart from the hard-switching converters, soft-switching topologies, such as LLC resonant converters and optimized advanced control techniques, have been adopted to achieve these design criteria. The LLC resonant converters have become an enticing choice for their capability of operating at high frequency, while achieving high power density under a wide input voltage range in renewable energy system applications [11]-[13]. Due to their ability of zero voltage switching, they achieve lower switching losses.

In prior art, numerous configurations of resonant converters with integrated PV systems and battery storage as multiport structures have been proposed. A half-bridge LLC resonant converter was presented in [14]. This topology includes two inputs that are connected to one PV and one battery storage system. A non-isolated resonant multiport switched capacitor was proposed in [15] for renewable sources and battery storage. A combined PWM and fixed frequency modulation strategy was used to regulate the output power and the voltages of the system. Contrary to the converter in [15], an isolated three-port LCL resonant converter was introduced in [16] for power sharing between the PV and the battery storage to the load. In [17], another LLC topology was proposed in which the LLC tank is shared between the two energy sources. While these configurations enable simultaneous power sharing between the input ports and may use fewer switches, they use a high number of passive components which increases the cost and size of the system. Due to the inability to transfer power from the load port back to the input ports in these multiport structures, the bidirectional system becomes more favorable for multi-source applications.

A multiport LLC resonant converter was presented in [18]-[20] for transferring power among all the ports. However, the three-winding transformer and the increased number of semiconductor devices, inductors and capacitors augment the cost and increase the footprint of the converter. A symmetric resonant tanks bidirectional LLC converter with equal operating frequency on both sides was presented in [21]. The main goal of this structure was to increase the power density with minimal resonant components volume. An ancillary clamping switch with additional flying capacitors three-level resonant converter topology was presented in [22] for bidirectional power flow. The use of supplementary capacitors and switches contributes to the augmentation of the cost and the complexity of the system [23]. A bidirectional power sharing converter with automatic transition from output to input and an additional inductor was presented in [24]. However, the voltage gain ratio posed limitations on the variable switching frequency and the efficiency of the converter. To compensate for the problem of limited voltage-gain range of traditional LLC converters, a new topology for high efficiency under wide voltage gain was constructed in [25]. In [26] and [27], a buck-boost type LLC converter was presented to achieve soft-switching and to operate as a step up structure in forward power flow and a step down structure in reverse operation mode.

While these studies proposed converters that improve upon precursory research work, they are all focused exclusively on two-port applications. In the case of integrated hybrid systems, such as PV, battery storage and grid, the converter topology has at least three-ports and, as a requirement, the battery converter has to be bidirectional. This type of converter is typically developed by employing two LLC resonant converters or utilizing a three-winding transformer. In a very few number of researches, different construction of LLC resonant converter topologies has been presented to boost power density and efficiency while eliminating the three-winding transformer and /or the second converter [28], [29].

In this research, a bidirectional multiport LLC resonant converter for grid-connected systems is investigated as an extension of work done in [30] and [35]. Additionally, a zone based power management scheme and an MMPPT control technique are analyzed for the integration of the battery and PV system. The uniqueness of this research lies within the utilization of three unequal sources that are connected through the LLC resonant converter. The proposed unified converter topology and the control technique remove the requirement for either two transformers or a three-winding transformer and the DC-DC boost converter of the PV system. As a result, the footprint and efficiency of the converter and the transformer are significantly improved. The proposed design configuration and control methodologies were investigated in MATLAB/Simulink and the obtained results are presented.

2. Topology Description

The proposed converter configuration is shown Fig. 1. The system contains three main components: the PV system, the battery energy storage and the utility grid. The PV and the battery energy storage share a common DC bus V_{dc} which is considered either as an input or an output of the resonant converter based on its operation mode. The battery energy storage is configured through a bidirectional buck-boost converter and connected parallel to the PV to form the two ports of the bidirectional converter at node A. The utility grid forms the other port of the converter through the voltage source inverter. The power flows between node A and node B via the high frequency transformer. As seen in Fig. 1, the renewable energy source is denoted as V_{pv}, which is the voltage of the PV system. C_{pv} is the input capacitor, V_{bat} represents the voltage of the battery storage and L_{bat} is the inductance of the bidirectional buck-boost converter, which is configured through the switches Q_1 and Q_2. At node A and node B respectively, C_{dc} and C_o form the DC bus capacitor and V_{dc} and V_o can be taken as either the input or output DC voltage of the LLC resonant converter, depending on the operation mode. The switches P_1, P_2, P_3, P_4, S_1, S_2, S_3 and S_4 form the full bridges of the resonant converter. L_r is the resonant inductor, C_r is the resonant capacitor and L_m is the magnetizing

inductance of the high frequency transformer. The three-phase voltage source inverter is composed of the switches G_1 through G_6. Multiport isolated bidirectional DC-DC converter topology is obtained by connecting all the ports together.

2.1- Principle of operation of the proposed converter

In order to best utilize the PV system when it is generating power, the maximum power point tracking (MPPT) is enabled. The MPPT is obtained through the regulation of the battery energy storage system current. The grid-connected three-phase voltage source inverter can transport the power supplied by the PV and the battery storage to the grid or can provide power to the battery storage from the grid. The power can be a mixture of the PV system, the battery storage and/or the grid source. Thus, this converter configuration has the capability of operating in two modes, the forward and reverse modes. For both modes, four instances can be analyzed, as seen in Fig. 2.

A- Forward Mode

When the converter is operating in forward mode, where the power flow is from node A to node B, the power sharing can be categorized into three zones, as seen in Fig. 2 (a), (b) and (c).

In Zone-I, the power consumed by both the grid and the battery storage is directly supported by the PV system. In this zone, the switches Q_1 of the bidirectional buck-boost and S_1 through $S4$ of the bidirectional LLC converter remain inactive, as seen in Fig. 3. Therefore, it can be seen that the battery storage is constantly being charged by the supplied power of the PV system and it can be considered as a load. The voltage source inverter also exports the power generated by the PV system to the grid and follows its power reference.

In Zone-II, the grid is simultaneously receiving power from both the PV system and the battery storage. In this zone, the switches Q_2 of the bidirectional buck-boost and S_1 through S_4 of the bidirectional LLC converter are kept off, as seen in Fig. 4. Thus, the battery storage also becomes a supplier for the grid.

In Zone-III, the switches Q_2 of the bidirectional buck-boost and S_1 through S_4 of the bidirectional LLC converter remain off, as seen in Fig. 5. Therefore, the battery storage is the sole power provider of the grid. This scenario most often occurs at night when the PV system is not able to provide any power.

B – Reverse Mode

The converter is operating in reverse mode when the power flows from node B to node A. In this operation mode the power sharing can only be possible between the grid and the battery energy storage system, as seen in Fig. 2 (d). In the reverse mode of operation, the battery storage system becomes a consumer, as it is always being charged by the grid. The switches P_1 through P_4 and Q_2 are turned off while S_1 through S_4 become active, as demonstrated in Fig. 6.

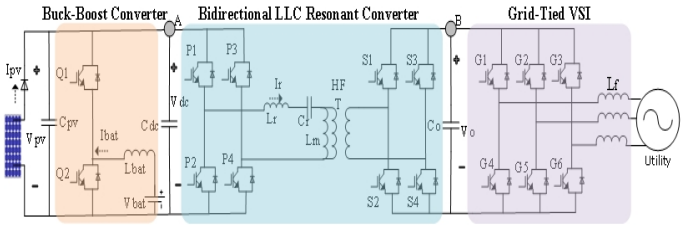

Fig. 1: The proposed multi-port resonant converter topology.

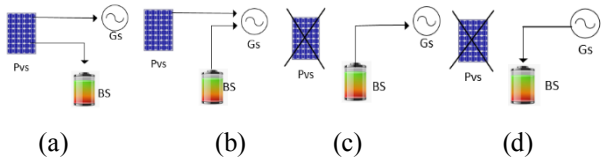

Fig. 2. Power flow characterization of the PV system (PVs), the battery system (BS) and the grid source (Gs): (a) Forward operation Zone-I (b) Forward operation Zone-II (c) Forward operation Zone-III (d) Reverse mode.

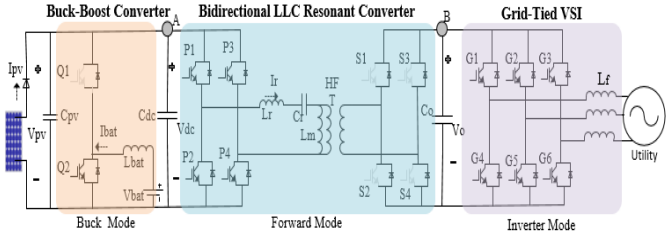

Fig. 3. Forward mode operation for Zone-I.

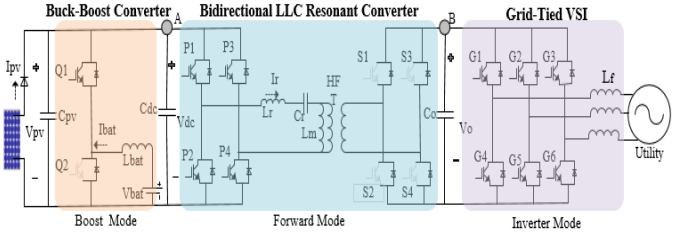

Fig. 4. Forward mode operation for Zone-II.

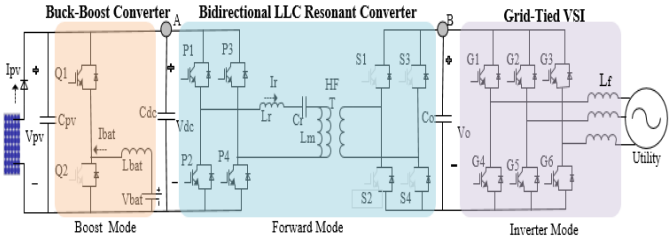

Fig. 5. Forward mode operation for Zone-III.

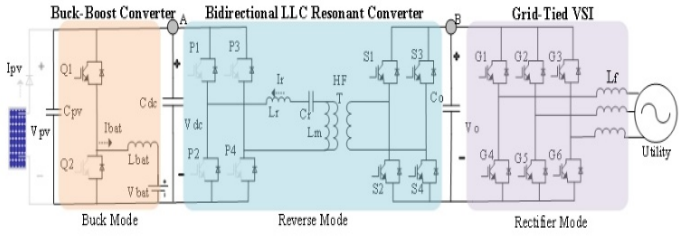

Fig. 6. Reverse mode operation.

3. DC Voltage Gain Characteristics of the Proposed Converter

An LLC resonant converter contains two resonant frequencies. The first resonance frequency is determined by the resonant inductor L_r, and the resonant capacitor C_r. The second resonant frequency is obtained using the two inductances of the transformers, the magnetizing inductance L_m and the resonant inductor L_r, and the resonant capacitor C_r. In these equations, f_{r1} and f_{r2} are the first and second resonance frequencies, respectively [31], [32] and [33]:

$$f_{r1} = \frac{1}{2\pi\sqrt{L_r C_r}} \quad (1)$$

$$f_{r2} = \frac{1}{2\pi\sqrt{(L_r+L_m)C_r}} \quad (2)$$

From the equivalent circuit models shown in Fig. 7, the DC gain of the LLC resonant converter can be obtained, as in equations (3) and (4) below, based on the theory of the Fundamental Harmonic Approximation (FHA) [27]:

$$K_{Forward} = \frac{aV_b}{V_a} = \frac{sL_m //R_o}{\frac{1}{sC_r}+ sL_r+ sL_m //R_o} \quad (3)$$

$$K_{backward} = \frac{aV_a}{V_b} = R_o + \frac{1}{sC_r} + sL_r + sL_m \quad (4)$$

To formulate simplified DC gain values for equations (3) and (4), the quality factor Q (the ratio of the square root of the resonance inductor and the capacitor to the effective resistance), m (the quotient of the sum of the primary inductance to the resonant inductance), the normalized frequency F_x (the fraction of the switching frequency to the first resonant frequency), the reflected load resistance value R_{ac}, and a (the turn ratio of the transformer) are calculated as follows:

$$Q = \frac{\sqrt{\frac{L_r}{C_r}}}{R_{ac}} \quad (5)$$

$$R_{ac} = \left(\frac{8}{\pi^2}\right)(a^2 \cdot R_o) \quad (6)$$

$$m = \frac{L_r + L_m}{L_r} \quad (7)$$

$$F_x = \frac{f_s}{f_{r1}} \quad (8)$$

The load resistance is considered to be a variable load, due to the fact the converter is not connected to a particular load. The typical values of the load resistance for both the forward and reverse operation modes can be formulated, as in (9) for power flow from node A to node B and (10) for the opposite direction, respectively:

$$R_o = \frac{V_o^2}{P_o} \quad (9)$$

$$R_o = \frac{V_{bus}^2}{P_{bat}} \quad (10)$$

Based on the considered convention in this paper, when the power is transferring from node A to node B, it is denoted as forward power transfer. When it flows from node B to node A, it is denoted as reverse power transfer. Therefore, two gain values were calculated from the previous equations and can be formulated into the following equations. Equation (11) is formulated for the forward operation and equation (12) for the reverse power transfer.

$$K(Q,m,F_x) = \frac{1}{\sqrt{\left[1+\frac{1}{m}\left(1-\frac{1}{F_x^2}\right)\right]^2+\left(F_x-\frac{1}{F_x}\right)^2 \cdot Q^2}} \quad (11)$$

$$K(Q,m,F_x) = \sqrt{1+\left(F_x-\frac{1}{F_x}\right)^2 . Q^2} \quad (12)$$

As obtained from (11) and (12), the gains of the LLC resonant converter can be controlled by regulating the switching frequency of the converter [27]. The gain path of the proposed converter design for several resistance values is demonstrated in Fig. 8 for both power operation modes.

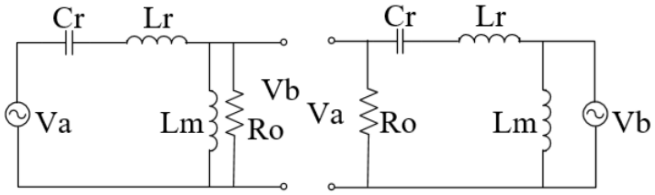

(a) (b)

Fig.7. Equivalent circuit models of a bidirectional LLC resonant converter. (a) Forward mode operation. (b) Reverse mode operation

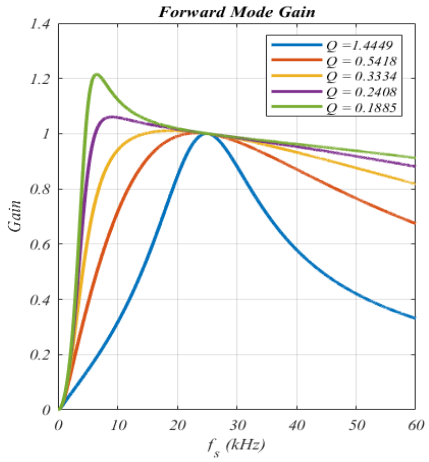

(a)

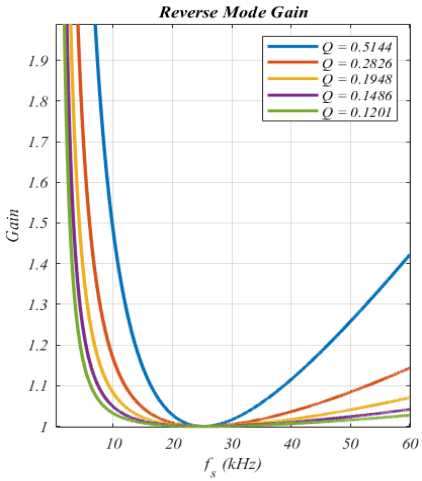

(b)

Fig. 8. DC gain of the bidirectional LLC converter for distinct Q values, a) Forward mode, b) Reverse Mode.

4. Control Technique for the Proposed System

The control strategy employed for the proposed structure has an objective of regulating the converter in both forward and reverse modes of operation. The derivation of the control method is based on Fig. 2 above and Fig. 9 below. In this work, 1Soltech 1STH-350-WH Monocrystalline PW Modules are used. The PV system is composed of 4 strings connected in parallel. Each string contains 19 PV modules that are connected in series. The MPPT curve for this PV connection is shown in Fig. 9. As it is presented in Fig.2, the description of the control method is as follows:

A- Zone-I and -II

In Zone-I and -II, when power is being transferred from node A to node B, it is imperative to extract the maximum power from the PV. To accomplish this, the MMPPT was derived from the well-known Incremental Conductance (IC) [34] theory to track the Maximum Power Point (MPP) of the PV in order to obtain the reference current for the battery.

At the instant when the solar irradiation intensity surpasses the preset lower irradiation boundary, the MMPPT is triggered and starts to regulate the reference current of the battery. Therefore, both the charging and the discharging current estimation are obtained from the PV system operating condition. When the operating point is on the right hand side of the MPP, the reference current of the battery is decreased. To achieve a reduced reference current of the battery, the power supplied by the battery can either be reduced or increased as dictated by the operation mode of the battery storage. Equation (15) depicts this condition.

Contrary to the right side, if the system operating point is on the left hand side of the MPP, the reference current of the battery is increased by the MMPPT. Therefore, the charging capacity can be increased or decreased. This method is presented in equation (14). When the operating point is at the MPP, the reference current of the battery is maintained constant by the MMPPT. This operation point is shown in equation (13).

$$\textit{At the MPP} \quad \frac{\Delta I}{\Delta V} = -\frac{I}{V} \Rightarrow Ibat^*(k) = Ibat^*(k-1) \qquad (13)$$

$$\textit{The left side} \quad \frac{\Delta I}{\Delta V} > -\frac{I}{V} \Rightarrow Ibat^*(k) = Ibat^*(k-1) - \Delta I \qquad (14)$$

$$\textit{The right side} \quad \frac{\Delta I}{\Delta V} < -\frac{I}{V} \Rightarrow Ibat^*(k) = Ibat^*(k-1) + \Delta I \qquad (15)$$

The flowchart describing the proposed MMPPT algorithm is given in Fig. 10. In Fig. 11, the performance of this control algorithm is shown. The solar irradiation trajectory and proportional reference current of the battery obtained by the MMPPT algorithm can be also seen. As previously explained, the MMPPT determines the battery current and state (charging or discharging) to maintain the operation of the PV at its MPP.

B- Zone-III

In Zone-III, the PV power is unavailable or is below the operating set point. The mode detector algorithm, as presented in Fig. 13, deactivates the MPPT technique and the battery storage is controlled in voltage regulation method. This can be seen in Fig. 13(a). During this period, a PI regulator is acquired to maintain the DC bus voltage at the desired level. The reference current of the battery is set by the PI regulator for maintaining a constant DC bus voltage.

In addition to the control techniques presented for Zone-I, -II and –III, the DC voltage, denoted V_o, of the full bridge LLC resonant converter is regulated by the variable switching frequency method in order to transfer power from node A to node B. In this mode of operation, the switches P_1, P_2, P_3 and P_4 are controlled and secondary side switches are disabled. Fig.13 (b) depicts this method.

C- Reverse Mode

In the reverse mode of operation, the battery energy storage system is supplied by the utility and the voltage source inverter works in rectification mode. In this operating condition, the mode detector method identifies the reference current of the battery, which was generated by another PI controller that regulates the voltage of battery. In contrast to the forward mode, the full bridge LLC resonant converter is controlled to keep the DC bus voltage (V_{dc}) at node A constant in the reverse mode. Upon activating the enable signal, the switches S_1, S_2, S_3 and S_4 on the secondary side of the transformer are switching and the switches P_1, P_2, P_3 and P_4 are turned off, as given in Fig. 13(b).

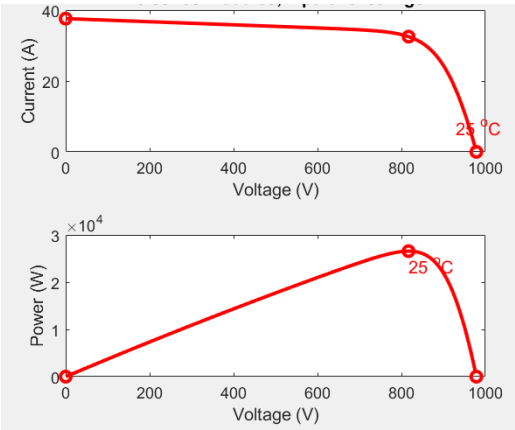

Fig. 9. The *I-V* and *P-V* curves

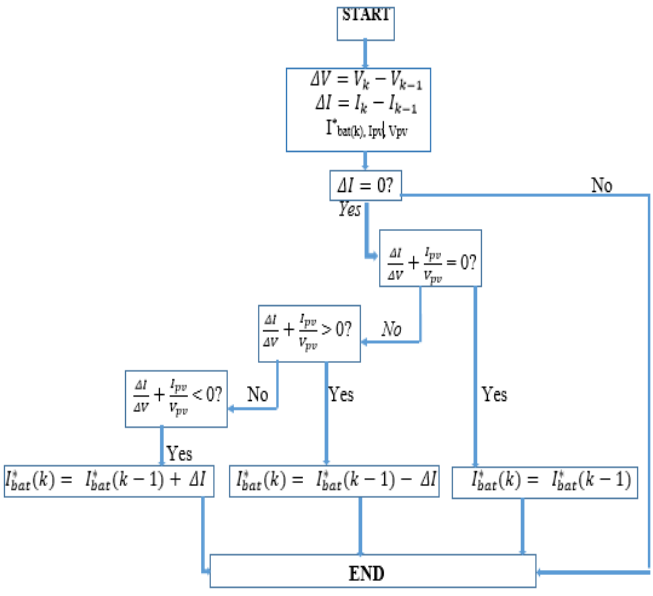

Fig. 10. Flowchart of the MMPPT controller

Finally, the cascaded controller, as seen in Fig.13 (b), is employed to manage the LLC resonant converter operation in both operating conditions. In the proposed control scenario, the current reference for the inner current loop is generated by the outer voltage control loop. The resonant current is filtered by a low pass filter whose cut-off frequency is designed to be equal to f_{r1}. In this topology, when power is being transferred from node A to node B, a higher level controller provides the active power reference for the voltage source inverter control system. The voltage source inverter is designed to operate at a power factor equal to one. Therefore, the reactive power is maintained constant for both operation modes. However, when power is being transferred from node B to node A, the active component of the current is obtained by a PI controller that is developed to keep the DC voltage V_o at its desired level. The synchronous reference frame current control method, given in Fig. 13(c), is applied to control the three-phase currents injected into the grid.

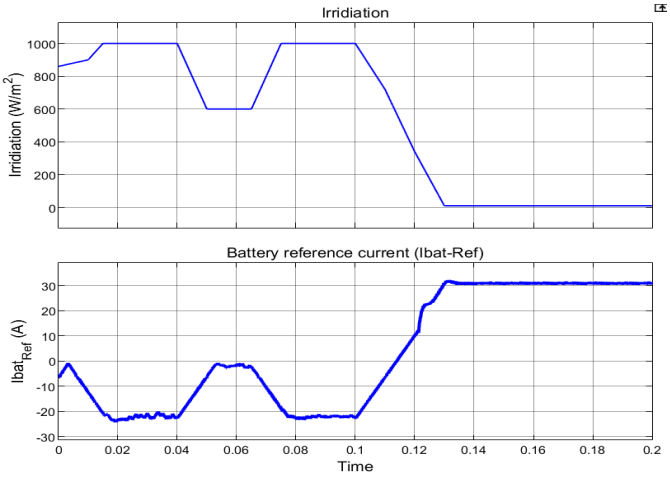

Fig. 11. MMPPT controller performance

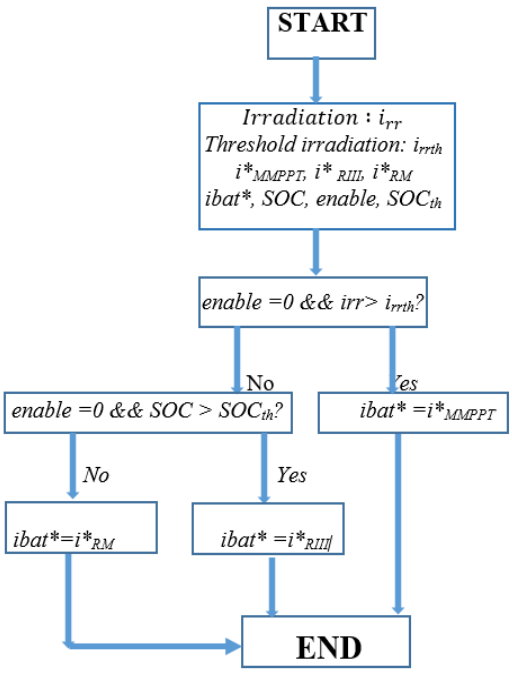

Fig. 12. Mode detector algorithm

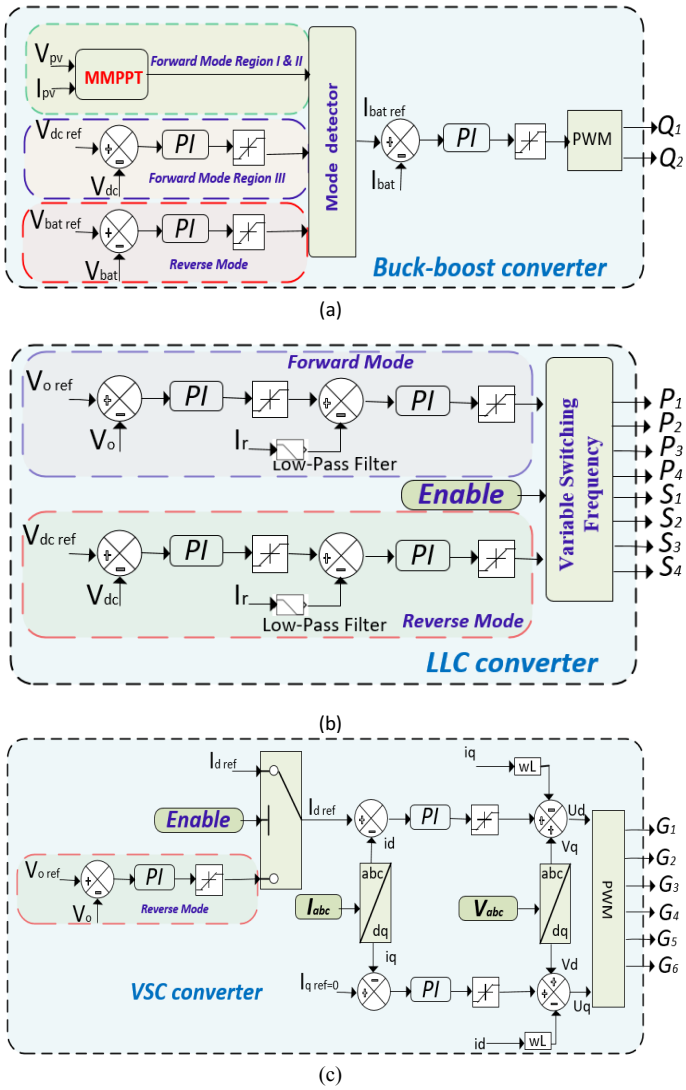

Fig. 13. Control of the proposed topology a) The MMPPT and battery charge/discharge controller b) The output voltage control (c) The voltage source inverter control

5. Simulation Results

In this research work, a bidirectional multiport LLC resonant converter structure and a control method including a MMPPT technique for tracking the MPP of the PV system are proposed for a grid-tied integrated battery-PV system. MATLAB/Simulink simulation analyses were carried out to examine the implementation of the proposed topology and control design. The complete configuration employs a bidirectional LLC resonant converter, a bidirectional buck-boost converter and a grid-connected voltage source inverter. The parameters of the proposed system are given in Table 1.

When power is being transferred from node A to node B, the *d*-axis current, which defines the active power of the voltage source inverter, is maintained constant at 20A, while *q*-axis current defining the reactive power remains constant at 0A. In Zone-I, it is observed that the power of the PV system is greater than the power fed to the grid. Therefore, the additional power supplied by the PV is stored in the energy storage unit. In Zone-II, the PV is not able to supply all the

power required by the grid. In such a scenario, the energy storage unit delivers the required power to stabilize the system. In Zone-III, the power of the PV system is zero. Therefore, the energy storage unit becomes the only power source for the grid. When power is being transferred from node B to node A, the grid supplies power to the energy storage unit.

Fig. 14 shows the voltage, current and power waveforms of the battery, the PV system and the grid for both operation modes and the three discussed zones. The power of the grid is designated by its mean value and the current of the grid by its root-mean-square value. Consequently, a slope can be observed during their variations.

Fig. 14 also demonstrates that after a small oscillation around the MPP, the MMPPT dictates the reference current of the battery for the current regulator of the bidirectional buck-boost converter. Therefore, regulating the battery current enables the PV system to operate at its MPP. Meanwhile, the bidirectional LLC resonant converter maintains the DC voltage of node B at the desired value and sets the DC bus for the voltage source inverter. The inverter can then transfer power to the three-phase AC utility grid.

At t=0.1s, it can be noticed that the irradiation intensity and the PV power begin to reduce. The MMPPT then controls the current reference of the battery to preserve the PV system at MPP. At the time the PV power is lower than the preset boundary, the MMPPT is deactivated and the battery current is regulated to keep the V_{dc} constant. In this zone (Zone-III), the battery storage becomes the sole power provider. The bidirectional LLC resonant converter remains controlled to maintain the voltage at node B (V_o) constant. In Zone-I, -II, and -III, the battery current is the principal varying parameter that manages the system. When the system is operating under power transfer from node B to node A in reverse mode, the battery is being supplied by the grid. As presented in Fig. 14, the proposed converter structure provides excellent performance in all operating conditions and a smooth switch between the operation modes.

The three-phase grid currents and voltages are presented in Fig. 15. Before t=0.2s, the voltage source inverter transfers power to the grid from the PV and/or battery system. From t=0s to t=0.2s, a higher level controller is assumed for providing a current reference of 20A to the voltage source inverter. At t=0.2s, the inverter changes its operation mode from supplying the grid to supplying the battery. In this operating condition, the reference current value is set by a PI regulator, which was designed to maintain the DC bus voltage of the inverter, which is also V_o at the desired level (800V). Therefore, some variations can be observed in the grid current after the transition.

In real application, the maximum current value is usually set to a certain threshold to protect the hardware. In this study, the peak current value is set to 30A. In a similar fashion, the battery charge current is also limited to 20A. As demonstrated in Fig. 15, the inverter exhibits fast transient behavior and excellent steady state performance in both operating conditions. Three-phase currents are all in sinusoidal waveforms and the total harmonic distortion (THD) value is 1.35% and 1.27% for the inverter and rectifier modes of operation, respectively.

The voltage, current and state of the charge (SOC%) of the battery storage unit are presented in Fig. 16. The initial SOC value is 30%. The battery is in charging mode in Zone-I and reverse mode. It is in discharging mode in Zone-II and -III. The operation of the proposed configuration can also be identified in this figure for each operation zone. Fig. 17 shows the primary and secondary voltages and the leakage currents of the LLC resonant converter for both modes of operation.

Table1. System Parameters

Parameters	**Value**
Resonant inductor, L_r	10µH
Magnetizing inductor, L_m	250µH
Resonant capacitor, C_r	4µF
Switching frequency (LLC resonant converter)	20-60kHz
Switching frequency (Buck-Boost Converter)	30 kHz
Switching frequency (VSI)	10 kHz
Output voltage, V_o	800V
Battery voltage, V_{bat}	460-540V
Grid voltage (phase to neutral, rms) and frequency, V_g,f_g	230V/50Hz
Inductance (Buck-Boost Converter), L_{bat}	0.7mH
VSI output filter, L_{inv}	2mH

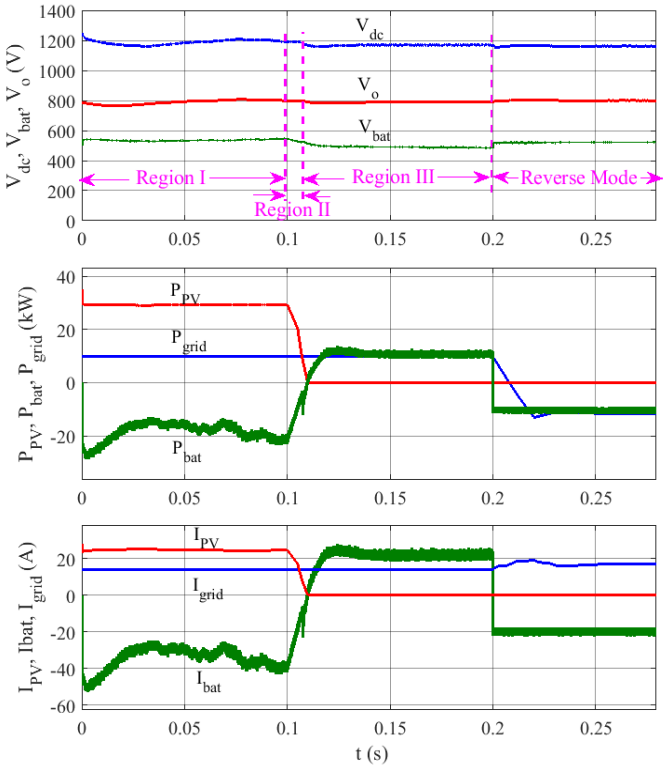

Fig. 14. Operation waveforms of the proposed system for all three regions and reverse mode.

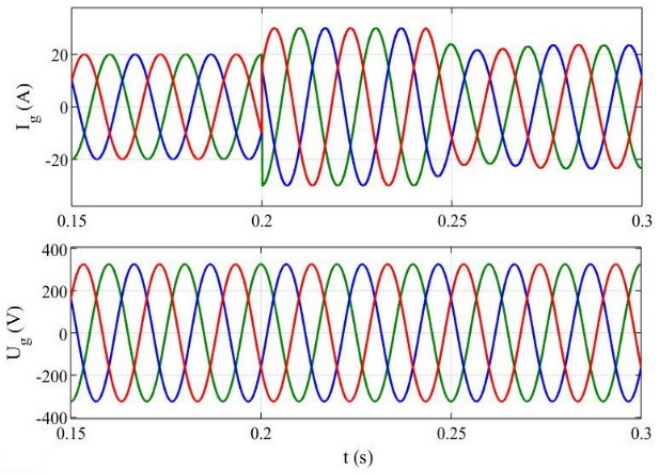

Fig. 15. Three-phase grid currents and voltages.

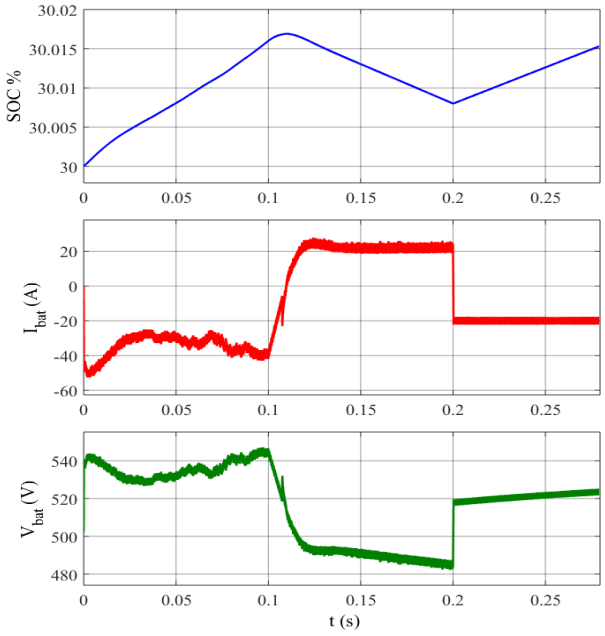

Fig. 16. The battery voltage, current and state of charge values.

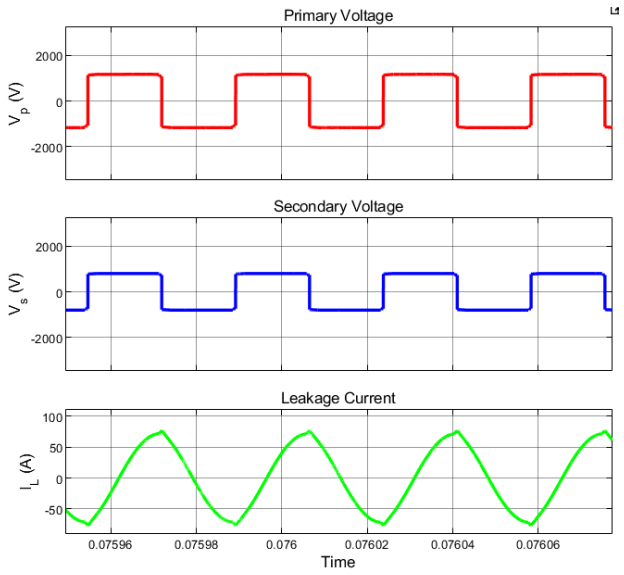

(a)

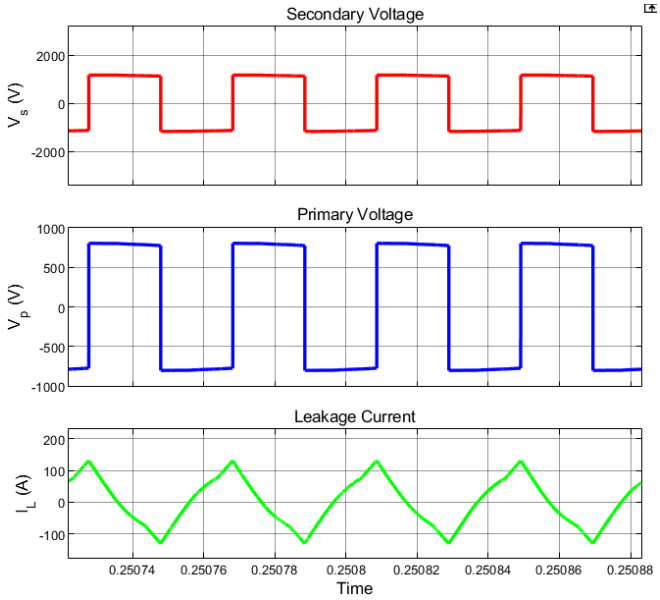

(b)

Fig. 17. Primary and secondary voltages and leakage currents of the converter (a) Forward mode (b) Reverse Mode

6. Conclusion

In this research work, a multiport bidirectional LLC resonant converter is provided for grid-connected PV and battery systems. The PV system is directly connected to the LLC resonant converter port at node A, while the battery is also connected to the same node via the bidirectional buck-boost converter. Additionally, the three-phase voltage source inverter is used to enable power transfer between node A and B and the three-phase AC grid. A control technique is implemented to manage the power flow between the ports and to regulate the voltages and currents of the proposed system for all operation modes. It is demonstrated that the proposed structure works in both operation modes, including all three zones, successfully. Additionally, the power flow between the ports is stable and accurate and the main voltage values at every port are maintained constant for any operation mode. The proposed system can combine two sources with only one transformer and provides galvanic isolation to the grid. Thus, it improves the power density and efficiency.

Acknowledgements

Dr. Necmi Altin thanks financial support from the Scientific and Technological Research Council of Turkey (TUBİTAK) BIDEB-2219 Postdoctoral Research Program.

References

[1] H. Tao, A. Kotsopoulos, J. L. Duarte and M. A. M. Hendrix, "Family of multiport bidirectional DC-DC converters," IEE Proceedings - Electric Power Applications, vol. 153, no. 3, pp. 451-458, 1 May 2006

[2] T. Labella, W. Yu, J.-S. Lai, M. Senesky, and D. Anderson, "A bidirectional-switch-based wide-input range high-efficiency isolated

resonant converter for photovoltaic applications," IEEE Trans. Power Electron., vol. 29, no. 7, pp. 3473–3484, 2014.

[3] M.-H. Ryu, H.-S. Kim, J.-H. Kim, J.-W. Baek, and J.-H. Jung, "Test bed implementation of 380V DC distribution system using isolated bidirectional power converters," 2013 IEEE Energy Conversion Congr. and Exposition, 2013.

[4] H. Tao, A. Kotsopoulos, J. L. Duarte, and M. A. M. Hendrix, "Transformer-coupled multiport ZVS bidirectional DC–DC converter with wide input range," IEEE Transactions on Power Electronics, vol. 23, no. 2, pp. 771–781, 2008.

[5] Z. Qian, O. Abdel-Rahman and I. Batarseh, "An Integrated Four-Port DC/DC Converter for Renewable Energy Applications," IEEE Transactions on Power Electronics, vol. 25, no. 7, pp. 1877-1887, July 2010.

[6] Phattanasak, Matheepot, Roghayeh Gavagsaz-Ghoachani, Jean-Philippe Martin, Babak Nahid-Mobarakeh, Serge Pierfederici, and Bernard Davat. "Control of a Hybrid Energy Source Comprising a Fuel Cell and Two Storage Devices Using Isolated Three-Port Bidirectional DC–DC Converters." *IEEE Transactions on Industry Applications* 51, no. 1 (2015): 491–97.

[7] Z. Ding, C. Yang, Z. Zhang, C. Wang, and S. Xie, "A novel soft-switching multiport bidirectional DC–DC converter for hybrid energy storage system," IEEE Transactions on Power Electronics, vol. 29, no. 4, pp. 1595–1609, 2014.

[8] Al-Atrash, Hussam, Feng Tian, and Issa Batarseh. "Tri-Modal Half-Bridge Converter Topology for Three-Port Interface." *IEEE Transactions on Power Electronics* 22, no. 1 (2007): 341–45.

[9] Qian, Zhijun, Osama Abdel-Rahman, and Issa Batarseh. "An Integrated Four-Port DC/DC Converter for Renewable Energy Applications." *IEEE Transactions on Power Electronics* 25, no. 7 (2010): 1877–87.

[10] Wu, Hongfei, Kai Sun, Runruo Chen, Haibing Hu, and Yan Xing. "Full-Bridge Three-Port Converters With Wide Input Voltage Range for Renewable Power Systems." *IEEE Transactions on Power Electronics* 27, no. 9 (2012): 3965–74.

[11] H. Hu, X. Fang, F. Chen, Z. J. Shen and I. Batarseh, "A Modified HighEfficiency LLC Converter With Two Transformers for Wide InputVoltage Range Applications," in IEEE Transactions on Power Electronics, vol. 28, no. 4, pp. 1946-1960, April 2013.

[12] X. Sun, X. Li, Y. Shen, B. Wang and X. Guo, "Dual-Bridge LLC Resonant Converter With Fixed-Frequency PWM Control for Wide Input Applications," IEEE Transactions on Power Electronics, vol. 32, no. 1, pp. 69-80, Jan. 2017.

[13] Y. Wei, N. Altin, Q. Luo and A. Nasiri, "A High Efficiency, Decoupled On-board Battery Charger with Magnetic Control", 2018 7th International Conference on Renewable Energy Research and Applications (ICRERA), Paris, 2018, pp. 920-925.

[14] S. Milad Tayebi, X. Chen, A. Bhattacharjee and I. Batarseh, "Design and Implementation of a Dual-Input LLC Converter for PV-Battery Applications," 2018 IEEE Energy Conversion Congress and Exposition (ECCE), Portland, OR, 2018, pp. 5934-5940.

[15] M. Uno and K. Sugiyama, "Switched capacitor converter-based multiport converter integrating bidirectional PWM and series-resonant converters for standalone photovoltaic systems", IEEE Transactions on Power Electronics, pp. 1–1, 2018.

[16] J. Zeng, W. Qiao, and L. Qu, "An isolated three-port bidirectional DCDC converter for photovoltaic systems with energy storage," 2013 IEEE Industry Applications Society Annual Meeting, 2013.

[17] T. Jiang, Q. Lin, J. Zhang and Y. Wang, "A novel ZVS and ZCS threeport LLC resonant converter for renewable energy systems," 2014 IEEE Energy Conversion Congress and Exposition (ECCE), Pittsburgh, PA, 2014, pp. 2296-2302.

[18] K. Tomas-Manez, Z. Zhang and Z. Ouyang, "Multi-port isolated LLC resonant converter for distributed energy generation with energy storage," 2017 IEEE Energy Conversion Congress and Exposition (ECCE), Cincinnati, OH, 2017, pp. 2219-2226.

[19] H. Krishnaswami and N. Mohan, "Three-Port Series-Resonant DC–DC Converter to Interface Renewable Energy Sources With Bidirectional Load and Energy Storage Ports," IEEE Transactions on Power Electronics, vol. 24, no. 10, pp. 2289-2297, Oct. 2009.

[20] E.-S. Kim, J.-H. Park, J.-S. Joo, S.-M. Lee, K. Kim, and Y.-S. Kong, "Bidirectional DC-DC converter using secondary LLC resonant tank", 2015 IEEE Appl. Power Electron. Conf. and Exposition (APEC), 2015.

[21] S. Zong, X. He, H. Luo, W. Li, and Y. Deng, "High-power bidirectional resonant DC–DC converter with equivalent switching frequency doubler", IET Renew. Power Gen., vol. 10, no. 6, pp. 834–842, Jan. 2016.

[22] T. Jiang, J. Zhang, Y. Wang, Z. Qian, and K. Sheng, "A bidirectional three-level LLC resonant converter with PWAM control", 2013 1st International Future Energy Electronics Conference (IFEEC), 2013.

[23] S. M. S. I. Shakib, S. Mekhilef, and M. Nakaoka, "Dual bridge LLC resonant converter with frequency adaptive phase-shift modulation control for wide voltage gain range", 2017 IEEE Energy Conversion Congr. and Exposition (ECCE), 2017.

[24] T. Jiang, J. Zhang, X. Wu, K. Sheng, and Y. Wang, "A bidirectional LLC resonant converter with automatic forward and backward mode transition", IEEE Trans. Power Electron., vol. 30, no. 2, 757–770, 2015.

[25] Y. Shen, H. Wang, F. Blaabjerg, A. A. Durra, and X. Sun, "A fixed-frequency bidirectional resonant DC-DC converter suitable for wide voltage range", 2017 IEEE Appl. Power Electron. Conf. and Exposition (APEC), 2017.

[26] C. Zhang, Z. Gao, and X. Liao, "Bidirectional DC–DC converter with series-connected resonant tanks to realize soft switching", IET Power Electronics, vol. 11, no. 12, pp. 2029–2043, 2018.

[27] E.-S. Kim, J.-H. Park, Y.-S. Jeon, Y.-S. Kong, S.-M. Lee, and K. Kim, "Bidirectional secondary LLC resonant converter using auxiliary switches and inductor", IEEE Appl. Power Electron. Conf. and Exposition, 2014.

[28] B. Mangu, S. Akshatha, D. Suryanarayana, and B. G. Fernandes, "Grid-connected PV-Wind-battery-based multi-input transformer-coupled bidirectional DC-DC converter for household applications," IEEE Trans. Emerg. Sel. Topics Power Electron., vol. 4, no. 3, pp. 1086–1095, 2016.

[29] J. Zeng, W. Qiao, and L. Qu, "An isolated three-port bidirectional DC-DC converter for photovoltaic systems with energy storage," 2013 IEEE Industry Applications Society Annual Meeting, 2013.

[30] G. Jean-Pierre, N. Altin, and A. Nasiri, "A Three-Port LLC Resonant Converter for Photovoltaic-Battery Hybrid System," 2019 IEEE Transportation Electrification Conference (ITEC), 2019.

[31] Y. Wei, N. Altin, Q. Luo, and A. Nasiri, "A high efficiency, decoupled on-board battery charger with magnetic control," 2018 7th International Conf. on Renewable Energy Research and Applications (ICRERA), 2018.

[32] Y. Wei, Q. Luo, X. Du, N. Altin, A. Nasiri and J. M. Alonso, "A Dual Half-bridge LLC Resonant Converter with Magnetic Control for Battery Charger Application," IEEE Trans. Power Electron. vol. 35, no. 2, pp. 2196-2207, Feb. 2020.

[33] Hiroyuki Haga, Hidenori Maruta, Fujio Kurokawa, "Analysis of Voltage Gain Tolerance due to the Resonant Circuit Variation of LLC Resonant Converter" 2016 International Conference on Renewable Energy Research and Applications (ICRERA).

[34] N. Altin and E. Ozturk, "Maximum power point tracking quadratic boost converter for photovoltaic systems," 2016 8th International Conference on Electronics, Computers and Artificial Intelligence (ECAI), 2016.

[35] G. Jean-Pierre, A. El Shafei, N. Altin, and A. Nasiri, "A Multiport Bidirectional LLC Resonant Converter for Grid-Tied Photovoltaic-Battery Hybrid System", 2019 International Conference on Renewable Energy Research and Applications (ICRERA), pp.1-6, Brasov, Romania, 2019.